

Measurement of Cytoplasmic Streaming in *Chara Corallina* by Magnetic Resonance Velocimetry

Jan-Willem van de Meent,^{1,2} Andy J. Sederman³, Lynn F. Gladden³, and Raymond E. Goldstein²

¹*Instituut-Lorentz/Leiden Institute of Physics, University of Leiden, Postbus 9506, 2300 RA, Leiden, NL*

²*Department of Applied Mathematics and Theoretical Physics, University of Cambridge, Wilberforce Road, Cambridge CB3 0WA, UK and*

³*Department of Chemical Engineering and Biotechnology, University of Cambridge, Pembroke Street, Cambridge CB2 3RA, UK*

In aquatic plants such as the Characean algae, the force generation that drives cyclosis is localized within the cytoplasm, yet produces fluid flows throughout the vacuole. For this to occur the tonoplast must transmit hydrodynamic shear efficiently. Here, using magnetic resonance velocimetry, we present the first whole-cell measurements of the cross-sectional longitudinal velocity field in *Chara corallina* and show that it is in quantitative agreement with a recent theoretical analysis of rotational cytoplasmic streaming driven by bidirectional helical forcing in the cytoplasm, with direct shear transmission by the tonoplast.

Keywords: *Chara corallina*, cytoplasmic streaming, magnetic resonance imaging.

Abbreviations: MRV, magnetic resonance velocimetry; MRI, magnetic resonance imaging; RF, radio-frequency

The pioneering work of Kamiya and Kuroda (Kamiya and Kuroda 1956) established that cytoplasmic streaming in Characean algae takes place not only in the cytoplasm, but also produces fluid flows that extend throughout the entire vacuole. As pointed out long ago (Pickard 1972) this result implies that the vacuolar membrane (tonoplast) efficiently transmits shear generated in the cytoplasm (Houtman et al. 2007) to the vacuole (Figure 1a). While the ability of membranes to flow under shear is well-known from the “tank-treading” of erythrocytes (Fischer et al. 1978), it is clear from recent studies of lipid vesicles under extensional flows (Kantsler et al. 2007) that sheared membranes can undergo instabilities that lead to complex dynamics. With the ability to image the dynamics of the tonoplast directly in *Arabidopsis* by means of a green-fluorescent-protein-labelled tonoplast integral channel protein (Cutler et al. 2000), there is fairly clear evidence that such complex dynamics do take place *in vivo*, and these may have implications for flows throughout the cell. In *Chara corallina*, for example, the actin-myosin system driving streaming is localized in two opposed helical bands at the cell periphery, and the regions of high shear where they meet may create complex tonoplast dynamics.

The possibility that streaming may impact on cellular metabolism by mixing the contents efficiently (Hochachka 1999, Pickard 2006) has been revisited recently through solutions of the coupled advection-diffusion dynamics of rotational cytoplasmic streaming (Goldstein et al. 2008, van de Meent et al. 2008). These calculations of velocities throughout the vacuole assumed that shear transmission by the tonoplast was complete, and showed that vacuolar flows can produce enhanced mixing, providing a possible mechanism for the homeostatic role hypothesized by Hochachka. The first direct measurements of the wall-to-wall profile are those of Kamiya and Kuroda (1956), who studied rhizoid cells, ‘leaf’ cells sprouting from nodes, and internodal cells, and found a constant velocity within the cytoplasm and a curved shear profile within the vacuole. Mustacich and Ware (1976) improved on these measurements by using laser-Doppler scattering through a chloroplast-free window obtained by exposure to an argon laser prior to observation. Pickard (1972) obtained velocity measurements for a collection of native particles in an internodal cell of *Chara braunii*, showing consistency with the velocity deduced under the approximation of non-helical indifferent zones.

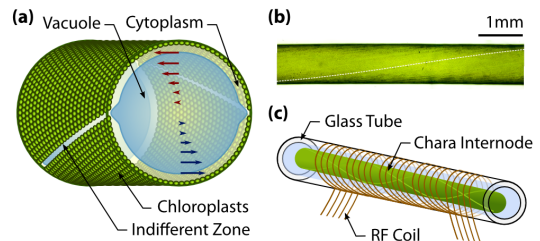


FIG. 1: Geometry of *Chara corallina*. (a) Cross-section of a *Chara* internode. Flow is driven in opposing directions along two helical bands separated by indifferent zones visible as light lines on the surface. Velocities are generated in a $10\ \mu\text{m}$ thick layer of cytoplasm at the periphery, but a shear flow extends into the central vacuole that takes up 95% of the volume of the cell. (b) Microscopy image of the sample prior to insertion into the glass tube. The dotted line shows a spiral of dimensionless wavelength $\lambda/R = 42$. (c) Schematic of sample holder enclosed in a horizontal RF coil. The length of the tube is 40 mm.

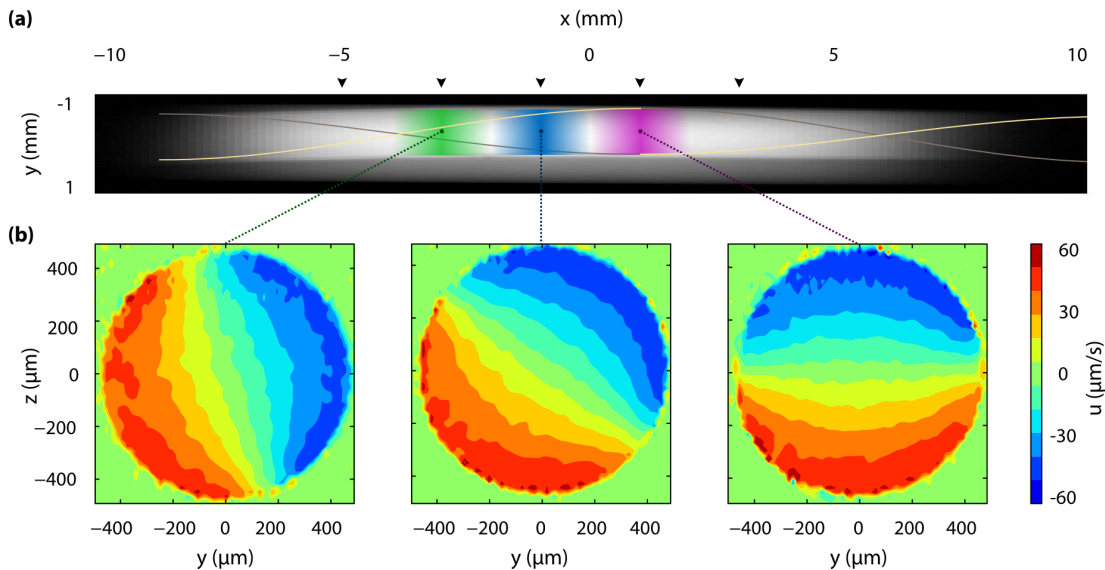


FIG. 2: MRV measurements of the cross-sectional velocity profile of *Chara corallina*. (a) NMR image of the sample, with the measurement volumes at $x = -3$ mm, -1 mm, 1 mm marked in green, blue and magenta. Dotted lines mark the extrapolated position of the indifferent zones, as determined from the orientation of the velocity profiles at 5 measurement points between $x = -5$ mm and $x = 3$ mm (marked with black arrowheads). (b) Cross-sectional plots of the velocity. The resolutions along the y - and z -axis are $16 \mu\text{m}$ and $31 \mu\text{m}$ respectively. Measurements were averaged along the x -axis over a Gaussian-weighted region of width 1 mm (full-width at half maximum). The fitted maximum velocities of the profiles are $45.2 \mu\text{m/s}$, $46.0 \mu\text{m/s}$ and $46.9 \mu\text{m/s}$.

Here we report a technical advance in the study of cytoplasmic streaming by obtaining the fluid velocity throughout a cross-section of internodal cells in *Chara corallina* directly with magnetic resonance velocimetry (MRV). Our results allow for quantitative tests of recent fluid dynamical theories (Goldstein et al. 2008, van de Meent et al. 2008) and suggest further uses for magnetic resonance imaging (MRI) in the study of large-scale streaming flows.

In recent years, MRI techniques have increasingly found use in non-medical applications (Elkins and Alley 2007), and the advent of phase-shift MRV has made it possible to perform non-invasive flow measurements on microscopic scales (Callaghan 1994). In MRV the initial application of a pulsed magnetic field gradient encodes each spin with a ‘label’ describing its position along the direction of the gradient. At a time Δ later (the “observation time”), a reversed gradient is applied, introducing a net phase shift in the orientation of the nuclear spin system that is directly related to the distance travelled in the direction of the gradient. By careful selection of the magnitude of the applied field gradients and the observation time, velocities from $\sim 10^{-5}$ – 10 m/s can be measured, depending on fluid properties. With sufficient time-averaging, spatial resolutions of 10 – $100 \mu\text{m}$ can be achieved, allowing imaging of biological systems on scales just slightly larger than those of typical single cells (Choma et al. 2006). While this technique has success-

fully been applied at tissue level in a variety of plant systems (Scheenen et al. 2001, Kckenberger 2004, Windt et al. 2006), it is in the uniquely sized internodal cells of *Chara* that we can obtain measurements of flows internal to single cells.

The Characean internode (Fig. 1a) is a single cylindrical cell with a diameter up to 1 mm and a length that can exceed 10 cm. The bulk of the volume of the cell is occupied by a large central vacuole, within which a 0.15 M concentration of salts results in the 5 bars of osmotic pressure that lends the cell its rigidity. A layer of cytoplasm $\sim 10 \mu\text{m}$ in thickness encloses the vacuole at the cell periphery. Charophytes are recognised as the highest genetic predecessors to vascular plants (Karol et al. 2001) and in *Chara* most organelles common to higher plants are found in the cytoplasm. Somewhat uniquely, the millions of chloroplasts cover the cell wall, packed into helical rows that spiral along the inner surface (Fig. 1a-b). On the inside of those rows, bundled actin filaments act as tracks for myosins that drag structures within the cell (Kachar 1985, Kachar and Reese 1988) and thereby entrain cytoplasm. With streaming rates as high as $100 \mu\text{m/s}$, the myosin XI found in *Chara* is the fastest known (Shimmen and Yokota 2004). As a result of a reversed polarity of the actin filaments, the flow is organised in two opposing bands, producing a “barber-pole” velocity at the cell periphery. These bands are separated by indifferent zones, identifiable by the absence of chloroplasts

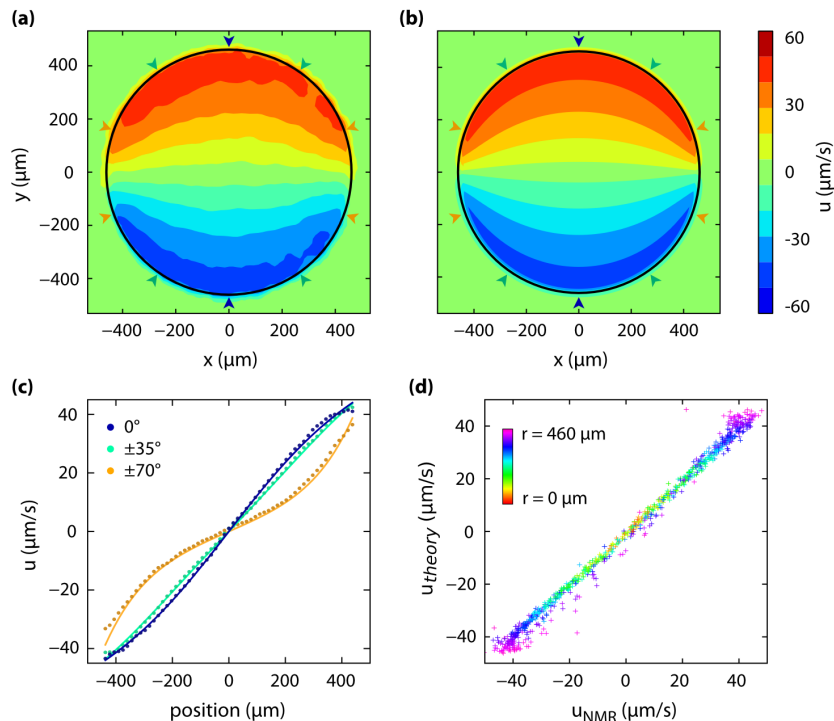


FIG. 3: Comparison between measurements and theoretical solution. (a) Reconstructed profile created by aligning and averaging the data sets shown in Figure 2b. The black circle shows the position of the cell wall. (b) Corresponding theoretical profile. (c) Three wall-to-wall velocity sections at orientations of 0° , $\pm 35^\circ$ and $\pm 70^\circ$ with respect to the z -axis (see arrowheads in panels above). For non-zero angles the data is averaged over the section with positive and negative orientation. Markers show the measured values, lines show the theoretical prediction. (d) Comparison between measurements and theoretical values. Data points from all three profiles are shown as markers, with the color of the marker denoting the radial position of the data. For clarity, only 1 in 10 points is shown.

and visible as two light lines crossing the surface of the cell.

To measure the cross-sectional flow inside the inter-nodal vacuole, a sample is inserted into a horizontal solenoidal radio-frequency (RF) coil (Fig 1c). Flow profiles with a cross-sectional resolution of $16 \mu\text{m} \times 31 \mu\text{m}$ are obtained over a total period of 192 – 256 minutes, averaging over a volume of 1 mm along the longitudinal axis of the cell (see Materials and methods). Figure 2a shows the location of the five averaging domains on a particular sample, and Fig. 2b shows the velocity profiles at three of those positions. Mean flow velocities are $\sim 45 \mu\text{m/s}$, typical of a cell of radius $R = 460 \mu\text{m}$ at the temperature of 298 K inside the coil (Pickard 1974). The helical pitch obtained from five short measurements 2 mm apart (Figure 2a, arrowheads), is $18.6^\circ/\text{mm}$, giving a dimensionless wavelength of $\lambda/R = 42.0$, in good agreement with our estimate from the light-microscopy image in Figure 1b.

Aligning and averaging the three datasets in Figure 2b we further enhance the signal to noise ratio of the profile. The resulting cross-section (Figure 3a) is in excellent agreement with the hydrodynamic solution presented in

earlier work (Goldstein et al 2008), shown in Figure 3b. In order to account for the $\sim 20^\circ$ of helical rotation along the averaging volume, we average the theoretical expression (see Materials and methods) over a length of 3 mm with the same Gaussian weighting as the MRV measurements. The wall-to-wall 1-dimensional profiles in Figure 3c show close agreement with the theoretical solution. In Figure 3d, measurement points are plotted against their theoretical values, in the manner of earlier velocity measurements (Pickard 1972). The color of the points indicates the radial distance from the centre of the cell. We see a remarkably good correspondence throughout the bulk of the cell, with deviations restricted primarily to points within a pixel from the cell wall, where partial-volume effects become significant.

In summary, we have shown that magnetic resonance velocimetry can yield detailed information on the velocity distribution of cytoplasmic streaming within single plant cells, allowing quantitative comparison with fluid dynamical theories. Natural extensions to this work include studies of other streaming geometries found in nature and of the spread of tracers as a probe of mixing (Esseling-Ozdoba et al. 2008).

Materials and methods

Plant materials

Chara corallina v. australis was obtained from the Botanic Garden of the University of Cambridge, courtesy of J. Banfield, and grown in a non-axenic culture, rooted in non-fertilized soil in a 100 liter tank filled with Artificial Pond Water (1 mM NaCl, 0.4 mM KCl, 0.1 mM CaCl₂). The tank was kept at room temperature and illuminated with a bench lamp on a 16/8 hour day-night cycle. During illumination, the light intensity at the top of the tank was ~ 250 lux. Samples of suitable size were placed in a Petri dish under a microscope to verify healthy streaming.

In preparation for measurements, the sample was inserted into a 3.0 mm outer diameter, 1.6 mm inner diameter glass capillary 40 mm in length, which was pre-filled with Forsberg medium (Forsberg 1965). The capillary tube was closed with PDMS plugs and a small volume of silicone grease to ensure a good seal.

Magnetic resonance velocimetry

Velocimetry experiments were performed on a Bruker Spectrospin DMX 200, 4.7 T magnet with a 20 mm long solenoid coil of diameter 3 mm. ¹H images were acquired at 199.7 MHz. Spatial resolution was achieved using 3-axis shielded gradient coils providing a maximum gradient strength of 49 G cm⁻¹ in each direction. Transport is measured over the observation time, Δ , and since the RMS displacement increases as $\Delta^{0.5}$ due to diffusion and as Δ^1 due to convection, for short Δ diffusive (incoherent) displacements can dominate over convective (coherent) ones, particularly in slowly convecting systems. Therefore, to weight the measurement towards the convective field a stimulated echo sequence was used to enable a large observation time for motion encoding. Further spatial imaging gradients were applied after the motion encoding to minimize diffusive attenuation. Hard 90° RF pulses were used except for the final pulse which was a Gaussian-shaped selective 90° RF pulse 512 μ s in duration. Experimental parameters used for the velocity images were: observation time, $\Delta = 500$ ms; velocity gradient duration, $d = 1.62$ ms; gradient increment, $g_{\text{inc}} = 10$ G cm⁻¹; number of velocity gradient increments, 2; recycle time, $TR = 1.9$ s; number of scans = 16; field-of-view = 2 mm \times 2 mm; pixel array size $N_{\text{read}} \times N_{\text{phase}} = 128 \times 64$; in-plane spatial resolution = 16 μ m \times 31 μ m; slice thickness = 1 mm; measurement duration = 64 min.

For each data set in Figure 2b, 4 measurements were taken between 3 and 7 hours apart and subsequently averaged. A Gaussian smoothing with 31 μ m FWHM was selectively applied to the streaming region whilst avoiding blurring at the cell periphery. The streaming velocity in the individual measurements was not observed to vary significantly over the 15 hour period of acquisition. Throughout the measurements the temperature

was maintained at 298 K by a regulated airflow system.

Hydrodynamic solution

The hydrodynamic solution was obtained as a mode expansion of the equations for Stokes flow (Goldstein et al. 2008). The system of equations assumes an infinitely long helical cell, allowing simplification of the problem to a 3-dimensional flow with symmetry, where the velocity depends only on the radial coordinate r and a helical angle $\varphi = \theta - (2\pi/\lambda)x$. Here, θ is the polar angle in the yz -plane and λ is the wavelength of the helical bands.

The solution of the flow problem can be expressed as a sum over a series of modes $f_i(r)\sin((2i+1)\varphi)$, with the radial modes $f_i(r)$ given in terms of a sum of Bessel functions. In the results presented here, 64 modes were used for the expansion. The velocity at the boundary was taken piece-wise constant on the bands, with a smooth crossover at the indifferent zones given by $\tanh(\varphi/\epsilon)$ and $\tanh((\pi-\varphi)/\epsilon)$ respectively. The cross-over width used was $\epsilon = 11$ μ m.

To allow better comparison with the MRV measurements, a series of profiles was averaged along the x -axis over a length of 3 mm, using a Gaussian weighting with a spread of 1 mm full-width at half maximum.

Funding

This work was supported by the Engineering and Physical Sciences Research Council [DTA to J.W.vdM., EP/F047991/1 to A.J.S. and L.F.G.], the Biotechnology and Biological Sciences Research Council [BB/F021844/1 to R.E.G.], Leiden University [to J.W.vdM.], the Leverhulme Trust and the Schlumberger Chair Fund [to R.E.G.].

Acknowledgments

We are grateful to M. Polin, T.J. Pedley, C. Picard, and I. Tuval for numerous discussions.

References

- Callaghan, P.T. (1994) *Principles of Nuclear Magnetic Resonance Spectroscopy*. Oxford University Press, Oxford.
- Choma, M.A., Ellerbee, A.K., Yazdanfar, S. and Izatt, J.A. (2006) Doppler flow imaging of cytoplasmic streaming using spectral domain phase microscopy. *J. Biomed. Optics* 11:024014.
- Cutler, S.R., Ehrhardt, D.W., Griffiths, J.S. and Somerville, C.R. (2000) Random GFP::cDNA fusions enable visualization of subcellular structures in cells of *Arabidopsis* at a high frequency. *Proc. Natl. Acad. Sci. USA* 97: 3718-3723.
- Elkins, C.J. and Alley, M.T. (2007) Magnetic resonance velocimetry: applications of magnetic resonance imaging in the measurement of fluid motion. *Exp. Fluids* 43:823-858.
- Esseling-Ozdoba, A., Houtman, C., van Lammeren, A.A.M., Eiser, E. and Emons, A.M.C. (2008) Hydrody-

- dynamic flow in the cytoplasm of plant cells. *J. Microscopy* 231:274-283.
- Fischer, T.M., Stohr-Lissen, M. And Schmid-Schonbein, H. (1978) The red cell as a fluid droplet: tank tread-like motion of the human erythrocyte membrane in shear flow. *Science* 202:894-896.
- Forsberg, C. (1965) Nutritional Studies of Chara in Axenic Cultures. *Physiologia Plantarum* 18:275-290.
- Goldstein, R.E., Tuval, I. and van de Meent, J.W. (2008) Microfluidics of cytoplasmic streaming and its implications for intracellular transport. *Proc. Natl. Acad. Sci. USA* 105:3663-3667.
- Hochachka, P.W. (1999) The metabolic implications of intracellular circulation. *Proc. Natl. Acad. Sci. USA* 96:12233-12239.
- Houtman, D., Pagonabarraga, I. Lowe, C.P., Esseling-Ozboda, Emons, A.M.C., and Eiser, E. (2007) Hydrodynamic flow caused by active transport along cytoskeletal elements. *Europhys. Lett.* 78:18001.
- Kachar, B. (1985) Direct visualization of organelle movement along actin-filaments dissociated from Characean algae. *Science* 227:1355-1357.
- Kachar, B. and Reese, T.S. (1988) The mechanism of cytoplasmic streaming in Characean algal cells – sliding of endoplasmic-reticulum along actin-filaments. *J. Cell. Biol.* 106:1545-1552.
- Kamiya, N. and Kuroda, K. (1956) Velocity distribution of the protoplasmic streaming in *Nitella* cells. *Bot. Mag. Tokyo* 69:544-554.
- Kantsler, V., Segre, E. and Steinberg, V. (2007). Vesicle dynamics in time-dependent elongational flow: wrinkling instability. *Phys. Rev. Lett.* 99:178102.
- Karol, K.G. et al. (2001) The closest living relatives of land plants. *Science* 294:2351-2353.
- Köckenberger, W., De Panfilis, C., Santoro, D., Dahiya, P. and Rawsthorne, S. (2004), High resolution NMR microscopy of plants and fungi. *J. Microscopy* 214:182-189.
- Mustacich, R.V. and Ware, B.R. (1976) A study of protoplasmic streaming in *Nitella* by laser Doppler spectroscopy. *Biophys. J.* 16:373-388.
- Pickard, W.F. (1972) Further observations on cytoplasmic streaming in *Chara braunii*. *Can. J. Bot.* 50:703-711.
- Pickard, W.F. (2003) The role of cytoplasmic streaming in symplastic transport. *Plant, Cell. Environ.* 26:1-15.
- Pickard, W.F. (2006) Absorption by a moving spherical organelle in a heterogeneous cytoplasm: implications for the role of trafficking in a symplast. *J. Theor. Biol.* 240:288-301.
- Scheenen, T.W.J., Vergeldt, F.J., Windt, C.W., de Jager, P.S. and Van As, H. (2001) Microscopic imaging of slow flow and diffusion: a pulsed field gradient stimulated echo sequence combined with turbo spin echo imaging. *J. Mag. Res.* 151:94-100.
- Shimmen, T. and Yokota, E. (2004) Cytoplasmic streaming in plants. *Curr. Op. Cell Biol.* 16:68-72.
- van de Meent, J.W., Tuval, I. and Goldstein, R.E. (2008) Nature's microfluidic transporter: rotational cytoplasmic streaming at high Péclet numbers. *Phys. Rev. Lett.* 101:178102.
- Windt, C.W., Vergeldt, F.J., de Jager, P.A. and van As, H. (2006). MRI of long-distance water transport: a comparison of the phloem and xylem flow characteristics and dynamics in poplar, castor bean, tomato and tobacco. *Plant Cell & Envir.* 29:1715-1729.